Supplement of Atmos. Meas. Tech., 18, 3547–3568, 2025
https://doi.org/10.5194/amt-18-3547-2025-supplement

Atmospheric Measurement Techniques
Open Access
EGU

Supplement of

Interpretation of mass spectra by a Vocus proton-transfer-reaction mass spectrometer (PTR-MS) at an urban site: insights from gas chromatographic pre-separation

Ying Zhang et al.

Correspondence to: Lin Wang (lin_wang@fudan.edu.cn)

Additional description of GC set ups and procedures.

When the GC system collects a sample, the sample first passes through an oxidant trap that contains activated sodium sulfite to minimize the impact of artifact-generating oxidants, like ozone, on the preconcentration steps. After the oxidant trap, the sample is split to two separate channels for preconcentration, where only Ch1 is equipped with a water trap to remove excess water to avoid condensation in the preconcentration steps. For both Ch1 and Ch2, the sample is initially preconcentrated onto multi-bed sample traps (Markes International, Universal 1000, C3-BAXX-5070 glass tube). Following the collection onto the sample traps, the system goes through a post-collection water purge for 2 min by forward-flowing dry gas (ultra-high purity N_2) through the traps. The collected sample is then thermally desorbed from the sample traps to transfer the sample to the second stage of the preconcentration system, multi-bed focusing traps (Markes International, U-T15ATA-2S cold trap). After this second preconcentration event, each focus trap is flash heated to transfer the sample to the head of that channel's designated column.

The temperature profiles of the sample traps and the focus traps in the GC system in one typical cycle are also shown in Fig. 1. Taking Ch1 for instance, the sample traps were flushed with a high-purity helium gas at 20 $cm^3\ min^{-1}$ (sccm) and at the same time heated, i.e., at 570 s for EI-MS detection and at 2370 s for PTR-MS detection, respectively in the cycle, to fully desorb the captured VOCs. The sample trap heating initially ramped from 30 ℃ to 150 ℃ at a rate of 12 ℃/sec, and then from 150 ℃ to 300 ℃ at a rate of 2.5 ℃/sec. The sample traps were then held at 300 ℃ for 60 seconds and then cooled to 30 ℃ within 300 seconds. The desorbed organic molecules were transported using the same 20 sccm helium as a carrier gas to the focus traps where they were further pre-concentrated. The focus traps were flash heated to achieve a discrete thermal desorption of captured VOCs. Taking Ch1 for example, the heating processes started at 1075 s for EI-MS detection and at 2875 s for PTR-MS detection, respectively in the cycle. The focus traps were heated from 30 ℃ to 300 ℃ within 10 second, and then held at 300 ℃ for 30 second and then cooled to 30 ℃ to concentrate collected organics onto the head of the GC columns. At the beginning of every half hour (0–300 s and 1800–2100 s in the one-hour cycle), the focus traps underwent a second heating process as described above as a precautionary cleaning procedure to remove VOCs that might remain in the previous trapping process (e.g. low-volatility species outside of the analytical range).

The temperature profiles of the two columns are also shown in Fig. 1. The two chromatographic columns, housed in separate ovens, underwent a similar temperature program after the focus traps cooled down to 30 ℃. The temperature program consisted of four phases: initially from 35 ℃ to 100 ℃ at a rate of 39 ℃/min, then from 100 ℃ to 150 ℃ at a rate of 15 ℃/min and from 150 ℃ to 220 ℃ at a rate of 30 ℃/min, and lastly held at 220 ℃ for 60 seconds for Ch1 and for 150 seconds for Ch2, respectively. The columns were cooled down in 150 seconds and kept at 35 ℃ until the next heating process.

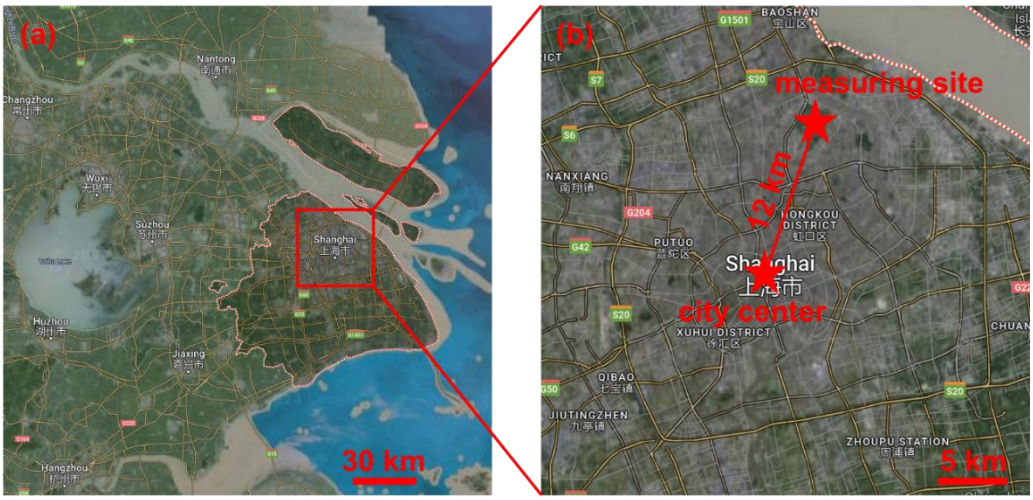

37 **Figure S1** The location of the measurement site as shown in a Google map (© Google Maps 2025).

38

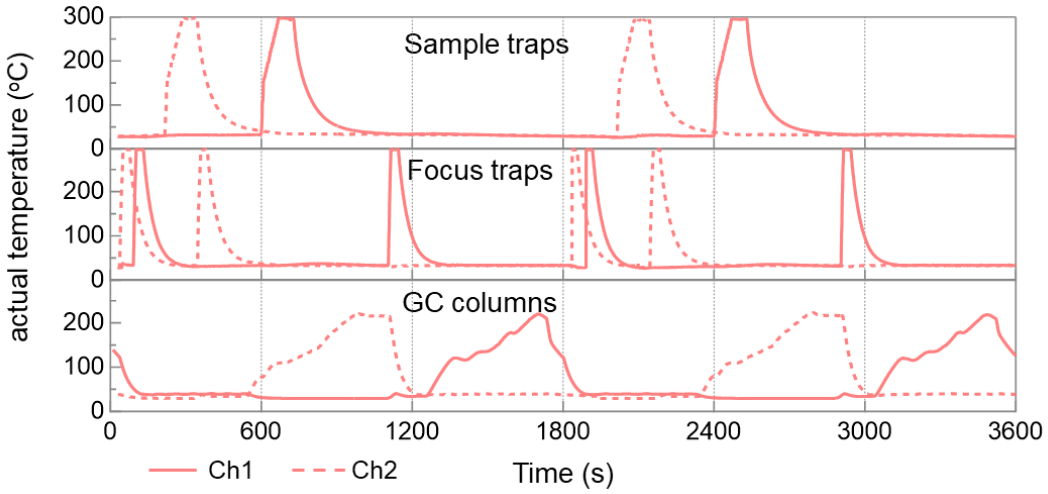

39 **Figure S2** Temperature profiles for the two-channel GC system (sample traps, focus traps, and GC
40 columns).

41

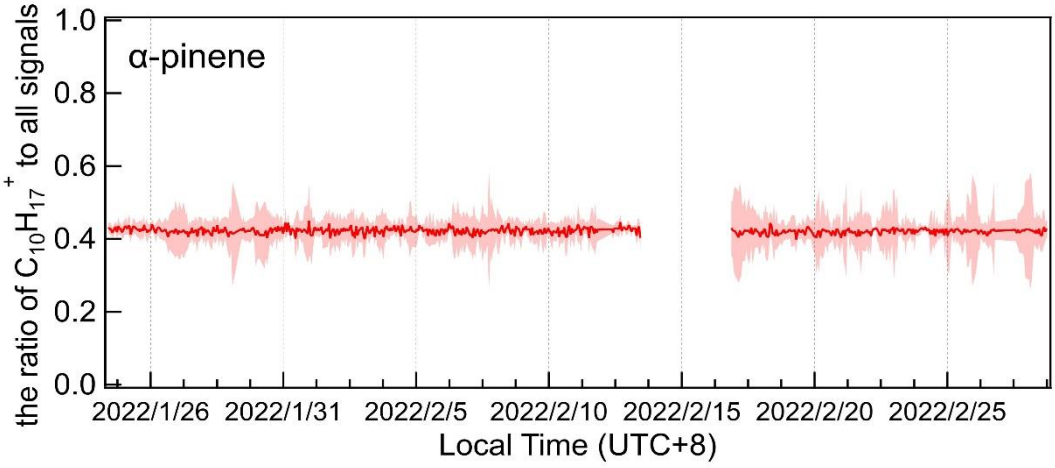

42 **Figure S3** The ratio of $C_{10}H_{17}^{+}$ signal to all signals for α-pinene during the measurement, suggesting an
43 estimated E/N of ~130 Td.

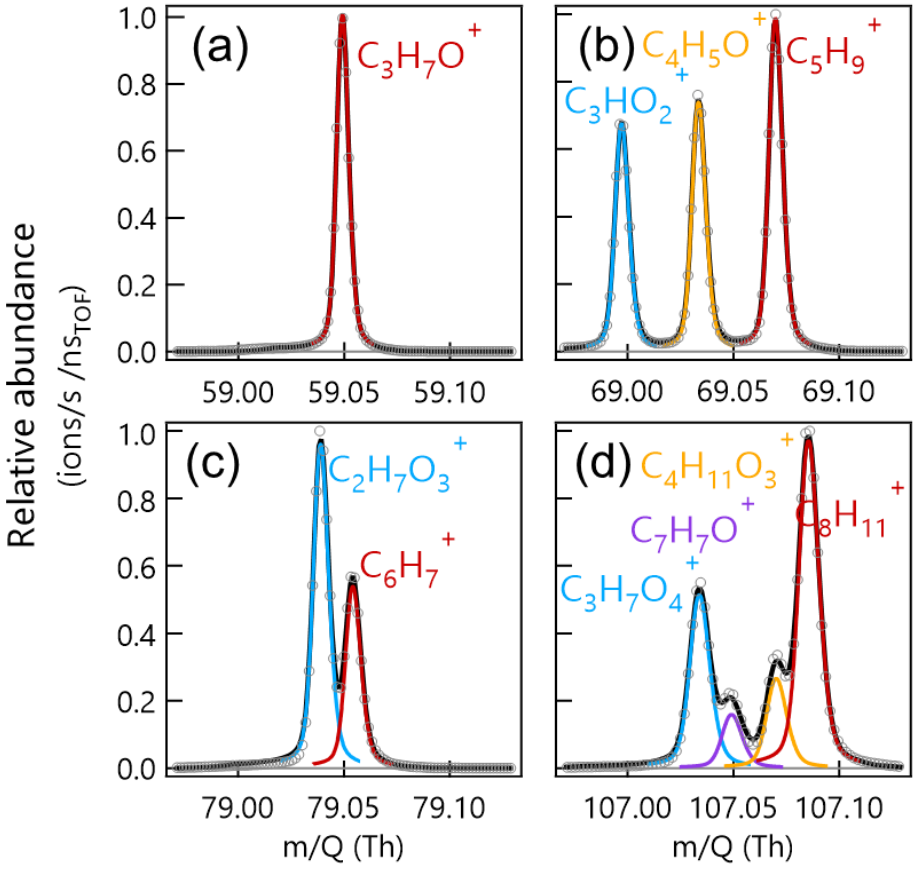

44 **Figure S4** High-resolution fitting of PTR signals at (A) ~59 Th, (B)~69 Th, (C)~79 Th, and (D)~107 Th,
45 respectively.

46

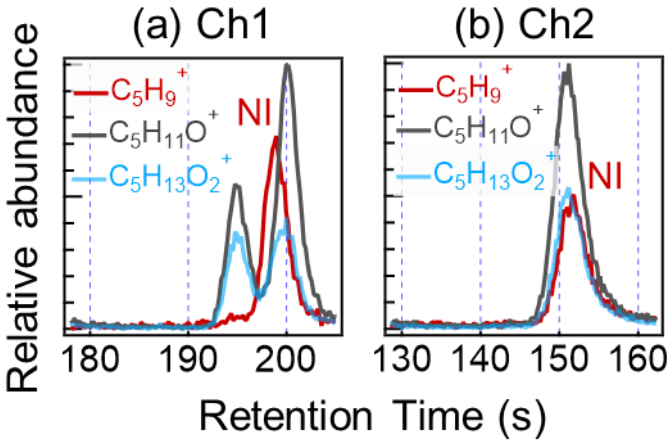

47 **Figure S5** The GC-PTR chromatograms for d-NI that produces $C_5H_9^+$ signals in the PTR measurement.

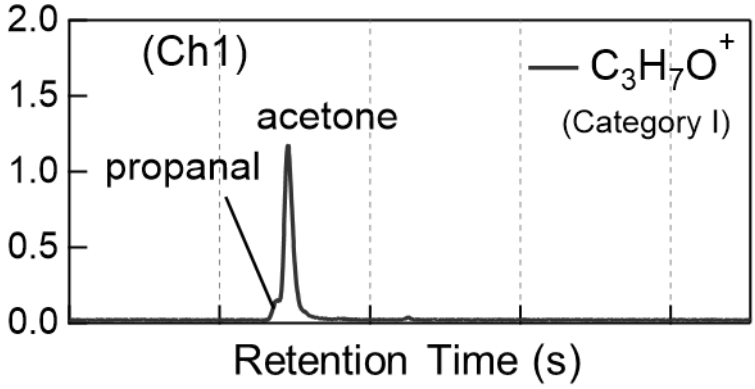

48 **Figure S6** A GC-PTR chromatogram of $C_3H_7O^+$, sampled from 7:26:46 to 7:35:07 on19 February 2022.
49

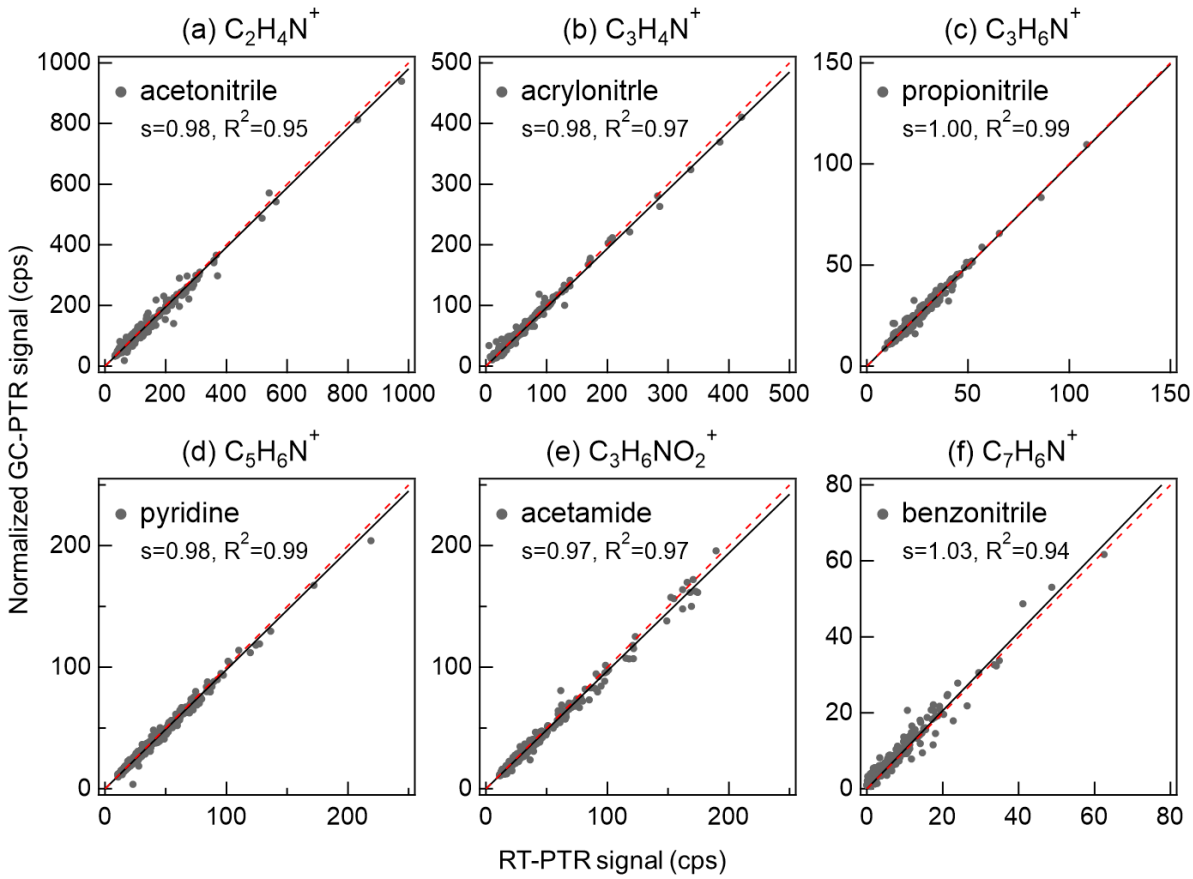

50 **Figure S7** Inter-comparison of PTR signals between RT-PTR and GC-PTR for N-containing species with
51 a time resolution of one hour. The GC-PTR signals are the average values of Ch1 and Ch2. s denotes the
52 slope of the linear fitting and R^2 denotes R square. The red dashed line is a 1:1 line for reference.
53

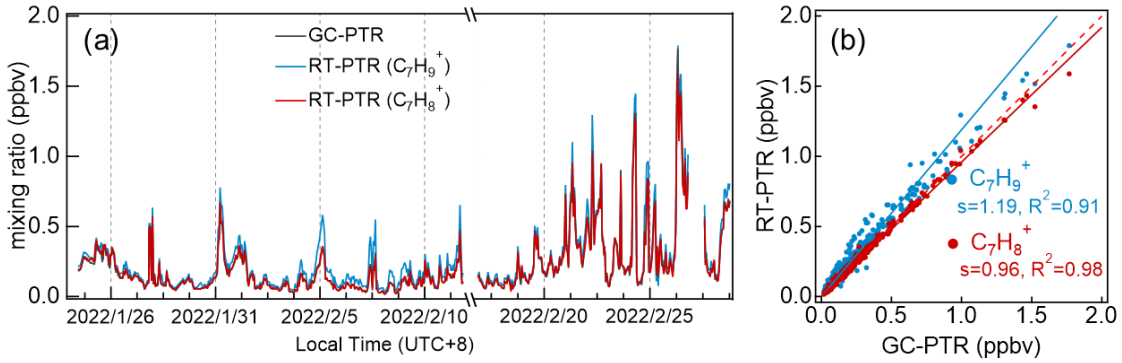

Figure S8 Inter-comparison of mixing ratios of toluene between GC-PTR measurements and RT-PTR measurements quantified by $C_7H_8^+$ and $C_7H_9^+$. The red dashed line denotes a 1:1 line for reference. The slope and R square are noted as s and R^2, respectively.

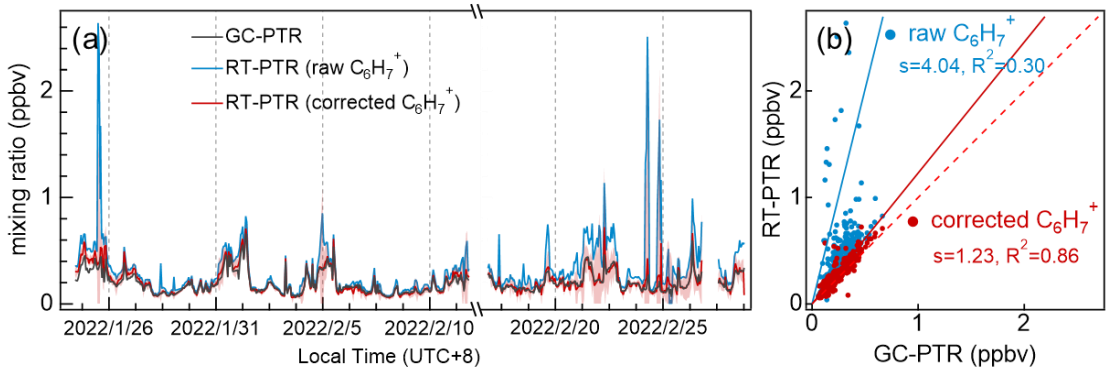

Figure S9 Inter-comparison of mixing ratios of benzene between GC-PTR measurements and RT-PTR measurements quantified by raw and corrected $C_6H_7^+$ signals. The red dashed line denotes a 1:1 line for reference. The slope and R square are noted as s and R^2, respectively.

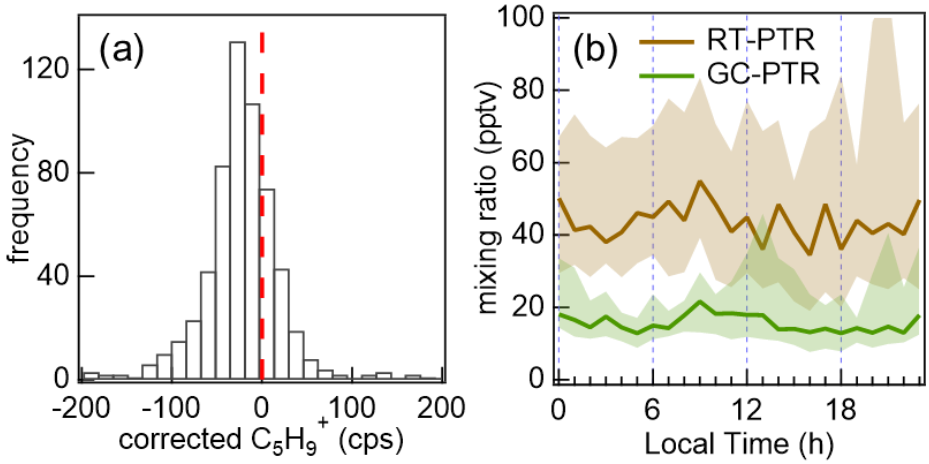

Figure S10 (A) Corrected $C_5H_9^+$ signals by RT-PTR for isoprene following the method developed by Matthew Coggon et. al. (2024). (B) Diurnal patterns of isoprene derived from RT-PTR and GC-PTR measurements, respectively. The solid lines denote the median values, and the shaded edges represent the upper and lower quartiles.

Table S1 Attribution of PTR signals to atmospheric species confirmed with the combination of GC and PTR-MS in previous studies.

m/z[a]	Signal ion	Main VOC identity	Interferences[b,c,d]				
			Utrecht (Gouw et al., 2003)	**Sonnblick** (Gouw et al., 2003)	**Boulder** (Warneke et al., 2003)	**Wisconsin** (Vermeuel et al., 2023)	**Las Vegas** (Coggon et al., 2024)
33	CH_4OH^+	methanol	NI	NI	NI	NR	NI
42	CH_3CNH^+	acetonitrile	NI	NI	NI	NR	NR
45	$C_2H_4OH^+$	acetaldehyde	NI	UI	UI	NR	ethanol
59	$C_3H_6OH^+$	acetone	propanal	NR	propanal	NR	propanal
63	$C_2H_6SH^+$	dimethyl sulfide	NR	NR	NR	NI	NR
69	$C_5H_8H^+$	isoprene	methylbutanals, pentenols	methylbutanals, pentenols	NR	heptanal, 1-nonene, octanal, and nonanal	methylbutanals, pentanal, octanal, and nonanal.
71	$C_4H_6OH^+$	C4 carbonyls	NR	NR	NR	NR	NI
79	$C_6H_6H^+$	benzene	NI	ethylbenzene	NI	NR	ethylbenzene benzaldehyde
93	$C_7H_8H^+$	toluene	NI	NI	NI	NR	ethyl-methyl-benzenes
105	$C_8H_8H^+$	styrene	NI	NR	NI	NR	NR
107	$C_8H_{10}H^+$ $C_7H_7O^+$	C8-aromatics benzaldehyde	NI	NI	NI	NR	NI
121	$C_9H_{12}H^+$	C9-aromatics	NI	NI	NI	NR	NI
137	$C_{10}H_{16}H^+$	monoterpenes	NR	NR	NR	NI	NR

Notes:

[a] PTR-MS was in a unit mass resolution (UMR) in the measurement launched in Utrecht, Sonnblick, and Boulder, and was in a high resolution in the measurement launched in Wisconsin and Las Vegas.

[b] NR stands for “not reported”.

[c] NI stands for “no interference”.

[d] UI stands for “unknown interference”.

Table S2. PTR signals of 63 ions that were detected in RT-PTR measurements but not detected in either channel of GC PTR system.

m/z	molecular formula	Note
19.0178	H_3O^+	reagent ion
29.9974	NO^+	reagent ion
31.9893	O_2^+	reagent ion
37.0284	$H_5O_2^+$	reagent ion
45.9924	NO_2^+	PANs related
55.0390	$H_7O_3^+$	reagent ion
73.0284	$C_3H_5O_2^+$	$C_xH_yO_z^+$
73.0495	$H_9O_4^+$	reagent ion
83.0128	$C_4H_3O_2^+$	$C_xH_yO_z^+$
84.0444	$C_4H_6NO^+$	/
85.0284	$C_4H_5O_2^+$	$C_xH_yO_z^+$
87.0077	$C_3H_3O_3^+$	$C_xH_yO_z^+$
89.0961	$C_5H_{13}O^+$	The protonated molecular ions ($C_5H_{13}O^+$) of the precursors ($C_5H_{12}O$ alcohols) may completely go through fragmentation in the PTR detection.
99.0441	$C_5H_7O_2^+$	$C_xH_yO_z^+$
101.0233	$C_4H_5O_3^+$	$C_xH_yO_z^+$
105.0182	$C_3H_5O_4^+$	$C_xH_yO_z^+$
109.0284	$C_6H_5O_2^+$	$C_xH_yO_z^+$
117.0546	$C_5H_9O_3^+$	$C_xH_yO_z^+$
119.0339	$C_4H_7O_4^+$	$C_xH_yO_z^+$
125.0233	$C_6H_5O_3^+$	$C_xH_yO_z^+$
127.0390	$C_6H_7O_3^+$	$C_xH_yO_z^+$
133.0495	$C_5H_9O_4^+$	$C_xH_yO_z^+$
135.0441	$C_8H_7O_2^+$	$C_xH_yO_z^+$
139.0390	$C_7H_7O_3$	$C_xH_yO_z^+$
141.0182	$C_6H_5O_4^+$	$C_xH_yO_z^+$
141.1638	$C_{10}H_{21}^+$	$C_xH_y^+$
145.0495	$C_6H_9O_4^+$	$C_xH_yO_z^+$
145.0859	$C_7H_{13}O_3^+$	$C_xH_yO_z^+$
145.1012	$C_{11}H_{13}^+$	$C_xH_y^+$
147.0288	$C_5H_7O_5^+$	$C_xH_yO_z^+$
147.0652	$C_6H_{11}O_4^+$	$C_xH_yO_z^+$
147.1016	$C_7H_{15}O_3^+$	$C_xH_yO_z^+$
151.0237	$C_4H_7O_6^+$	$C_xH_yO_z^+$
151.0390	$C_8H_7O_3^+$	$C_xH_yO_z^+$
151.0754	$C_9H_{11}O_2^+$	$C_xH_yO_z^+$
151.1481	$C_{11}H_{19}^+$	$C_xH_y^+$
153.0546	$C_8H_9O_3^+$	$C_xH_yO_z^+$

155.0339	$C_7H_7O_4^+$	$C_xH_yO_z^+$
155.0703	$C_8H_{11}O_3^+$	$C_xH_yO_z^+$
155.1067	$C_9H_{15}O_2^+$	$C_xH_yO_z^+$
157.0132	$C_6H_5O_5^+$	$C_xH_yO_z^+$
157.0859	$C_8H_{13}O_3^+$	$C_xH_yO_z^+$
159.0652	$C_7H_{11}O_4^+$	$C_xH_yO_z^+$
159.1016	$C_8H_{15}O_3^+$	$C_xH_yO_z^+$
161.0445	$C_6H_9O_5^+$	$C_xH_yO_z^+$
161.1172	$C_8H_{17}O_3^+$	$C_xH_yO_z^+$
165.0546	$C_9H_9O_3^+$	$C_xH_yO_z^+$
167.0339	$C_8H_7O_4^+$	$C_xH_yO_z^+$
167.0703	$C_9H_{11}O_3^+$	$C_xH_yO_z^+$
167.1067	$C_{10}H_{15}O_2^+$	$C_xH_yO_z^+$
167.1430	$C_{11}H_{19}O^+$	$C_xH_yO_z^+$
167.1794	$C_{12}H_{23}^+$	$C_xH_y^+$
169.0859	$C_9H_{13}O_3^+$	$C_xH_yO_z^+$
169.1223	$C_{10}H_{17}O_2^+$	$C_xH_yO_z^+$
173.1172	$C_9H_{17}O_3^+$	$C_xH_yO_z^+$
175.1329	$C_9H_{19}O_3^+$	$C_xH_yO_z^+$
175.1481	$C_{13}H_{19}^+$	$C_xH_y^+$
177.1638	$C_{13}H_{21}^+$	$C_xH_y^+$
183.2107	$C_{13}H_{27}^+$	$C_xH_y^+$
189.1121	$C_9H_{17}O_4^+$	$C_xH_yO_z^+$
189.1274	$C_{13}H_{17}O^+$	$C_xH_yO_z^+$
195.1227	$C_8H_{19}O_5^+$	$C_xH_yO_z^+$
209.1384	$C_9H_{21}O_5^+$	$C_xH_yO_z^+$

Table S3. PTR signals of 22 ions whose campaign-average relative differences between RT-PTR and GC-PTR were larger than 10% in both GC channels.

m/z	molecular formula	Note
41.0386	$C_3H_5^+$	$C_xH_y^+$
62.9632	$CClO^+$	/
69.0699	$C_5H_9^+$	$C_xH_y^+$
71.0855	$C_5H_{11}^+$	$C_xH_y^+$
77.0233	$C_2H_5O_3^+$	$C_xH_yO_z^+$
83.0491	$C_5H_7O^+$	$C_xH_yO_z^+$
99.0077	$C_4H_3O_3^+$	$C_xH_yO_z^+$
101.0597	$C_5H_9O_2^+$	$C_xH_yO_z^+$
116.9060	CCl_3^+	/
117.0182	$C_4H_5O_4^+$	$C_xH_yO_z^+$
119.0703	$C_5H_{11}O_3^+$	$C_xH_yO_z^+$
123.0441	$C_7H_7O_2^+$	$C_xH_yO_z^+$
123.0652	$C_4H_{11}O_4^+$	$C_xH_yO_z^+$
135.1016	$C_6H_{15}O_3^+$	$C_xH_yO_z^+$
141.0546	$C_7H_9O_3^+$	$C_xH_yO_z^+$
141.0910	$C_8H_{13}O_2^+$	$C_xH_yO_z^+$
143.0855	$C_{11}H_{11}^+$	$C_xH_y^+$
153.0910	$C_9H_{13}O_2^+$	$C_xH_yO_z^+$
153.1274	$C_{10}H_{17}O^+$	$C_xH_yO_z^+$
167.0550	$C_5H_{11}O_6^+$	$C_xH_yO_z^+$
171.1380	$C_{10}H_{19}O_2^+$	$C_xH_yO_z^+$
173.0808	$C_8H_{13}O_4^+$	$C_xH_yO_z^+$

Table S4 Species identification derived by the comparison between standard EI mass spectra and measured EI mass spectra, and between theoretical and measured retention times of GC elutes sampled from 16:56:46 to 17:05:07 on 19 February 2022. The theoretical retention time is calculated based on the Kovat's number [47].

	Channel 1					Channel 2				
	No.	**Identification**	**Match to standard EI mass spectrum**	**Theoretical retention time (s)**	**Measured retention time (s)**	**No.**	**Identification**	**Match to standard EI mass spectrum**	**Theoretical retention time (s)**	**Measured retention time (s)**
59.05491 Th $C_3H_7O^+$	a1	acetone	99%	/	45	a2	acetone	99%	32	31
107.0855 Th $C_8H_{11}^+$	b1	ethylbenzene	98%	299	301	b4	ethylbenzene	97%	226	225
	b2	m-xylene	95%	305	307	b5	p-xylene	95%	/	230
		and p-xylene	96%	306		b6	m-xylene	97%	233	233
	b3	o-xylene	97%	327	328	b7	o-xylene	98%	259	259
79.0542 Th $C_6H_7^+$	c1	benzene	99%	158	161	c8	benzene	99%	126	127
	c2	ethylbenzene	98%	299	301	c9	ethylbenzene	97%	226	225
	c3	p-xylene	95%	305	307	c10	p-xylene	97%	/	230
		and m-xylene	96%	306			and m-xylene	95%	233	233
	c4	o-xylene	97%	327	328	c11	isopropyl-benzene	94%	/	248
	c5	isopropyl-benzene	95%	344	345	c12	o-xylene	98%	259	259
	c6	n-propyl-benzene	96%	367	367	c13	n-propyl-benzene	95%	270	270
	c7	benzaldehyde	95%	403	402	c14	benzaldehyde	98%	458	456
69.0699 Th $C_5H_9^+$	d1	isoprene	96%	/	19	d3	octanal	95%	316	316
	d2	octanal	98%	404	405	d4	nonanal	96%	377	375
						d5	decanal	95%	425	422

References

Coggon, M. M., Stockwell, C. E., Claflin, M. S., Pfannerstill, E. Y., Xu, L., Gilman, J. B., Marcantonio, J., Cao, C., Bates, K., Gkatzelis, G. I., Lamplugh, A., Katz, E. F., Arata, C., Apel, E. C., Hornbrook, R. S., Piel, F., Majluf, F., Blake, D. R., Wisthaler, A., Canagaratna, M., Lerner, B. M., Goldstein, A. H., Mak, J. E., and Warneke, C.: Identifying and correcting interferences to PTR-ToF-MS measurements of isoprene and other urban volatile organic compounds, Atmos. Meas. Tech., 17, 801–825, https://doi.org/10.5194/amt-17-801-2024, 2024.

Gouw, J. de, Warneke, C., Karl, T., Eerdekens, G., Veen, C. van der, and Fall, R.: Sensitivity and specificity of atmospheric trace gas detection by proton-transfer-reaction mass spectrometry, Int. J. Mass Spectrom., 223, 365–382, https://doi.org/10.1016/s1387-3806(02)00926-0, 2003.

Vermeuel, M. P., Novak, G. A., Kilgour, D. B., Claflin, M. S., Lerner, B. M., Trowbridge, A. M., Thom, J., Cleary, P. A., Desai, A. R., and Bertram, T. H.: Observations of biogenic volatile organic compounds over a mixed temperate forest during the summer to autumn transition, Atmos. Chem. Phys., 23, 4123–4148, https://doi.org/10.5194/acp-23-4123-2023, 2023.

Warneke, C., Gouw, J. A. de, Kuster, W. C., Goldan, P. D., and Fall, R.: Validation of Atmospheric VOC Measurements by Proton-Transfer- Reaction Mass Spectrometry Using a Gas-Chromatographic Preseparation Method, Environ. Sci. Technol., 37, 2494–2501, https://doi.org/10.1021/es026266i, 2003.